Supporting Information: XRD spectra of MBG, FITC-MBG, MBG-FA, and FITC-MBG-FA, BET spectra of MBG, FITC-MBG, MBG-FA, and FITC-MBG-FA, IR spectra of MBG, MBG-FA, MBG/CTP, MBG-FA/CPT, CPT and FA. TGA trace of MBG, MBG/CPT, MBG-FA/CPT and MBG-FA/CPT. CLSM and bright field of FITC-MBG and FITC-MBG-FA. The IC50 value of CPT, MBG/CPT and MBG-FA/CPT. DLS of MBG. Flow of FITC-MBG and FITC-MBG-FA. N_2 absorption/desorption of MBG/CPT and MBG-FA/CPT.

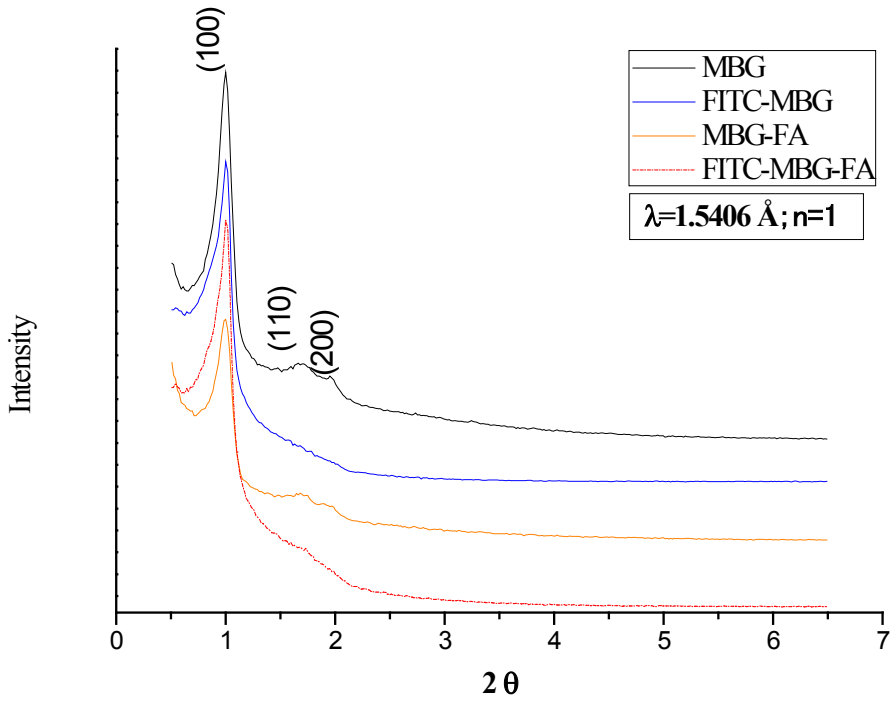

Figure S1. XRD spectra of MBG, FITC-MBG, MBG-FA, and FITC-MBG-FA.

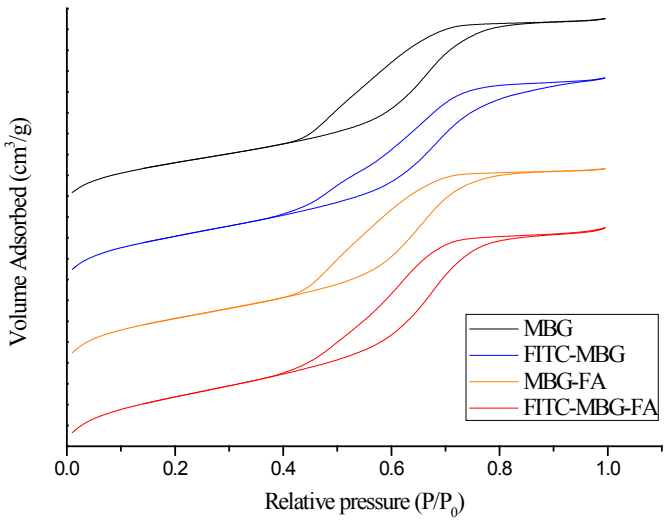

Figure S2. BET spectra of MBG, FITC-MBG, MBG-FA, and FITC-MBG-FA

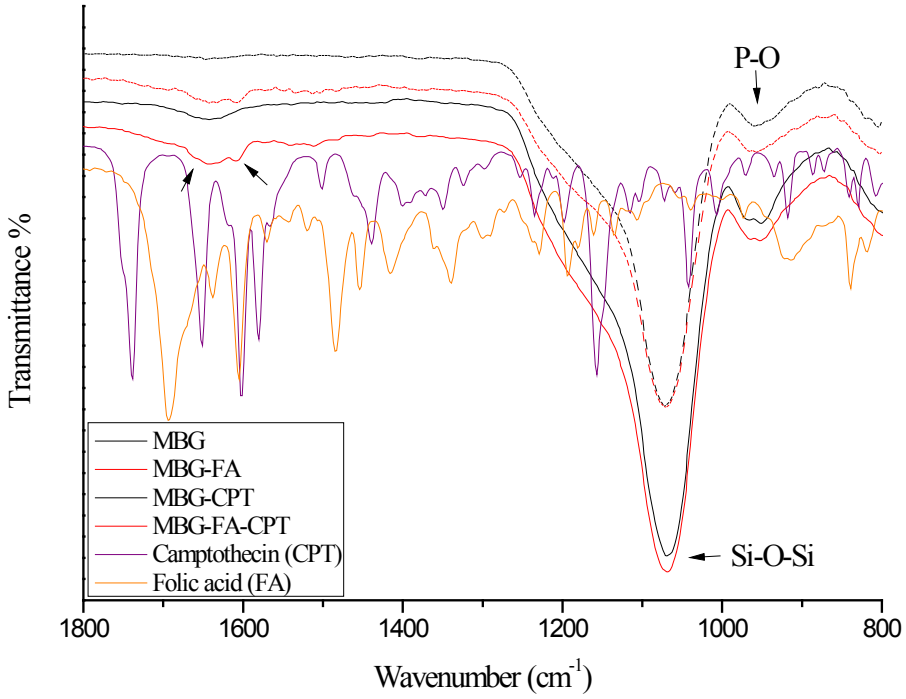

Figure S3. FT-IR spectra of MBG, MBG-FA, MBG-CPT, MBG-FA-CPT, Camptothecin (CPT), and Folic acid(FA).

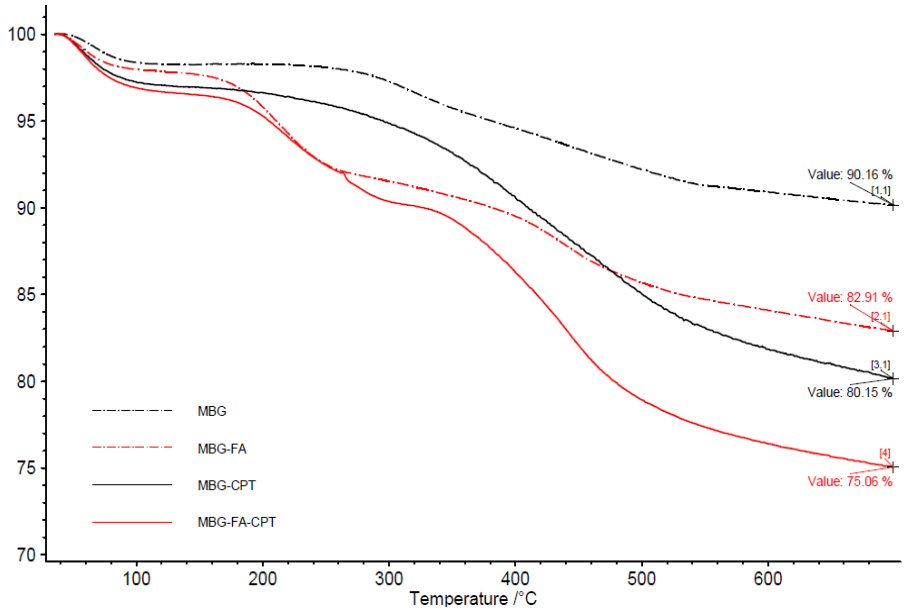

Figure S4. TGA trace of MBG, MBG/CPT, MBG-FA/CPT and MBG-FA/CPT.

We tested the endocytosis of MBG and MBG-FA on the bone tumor cell line (MG63), which is a FR^{-ve} cell line. Supporting Figures show the effects of MBG and MBG-FA on MG63 cell lines measured by CLSM. These MBG and MBG-FA were covalently linked with fluorescein isothiocyanate (FITC) to make them display green spots, comparing with supporting figure 5 and 6; it doesn't show a clear change of endocytosis after MBG grafted folic acid.

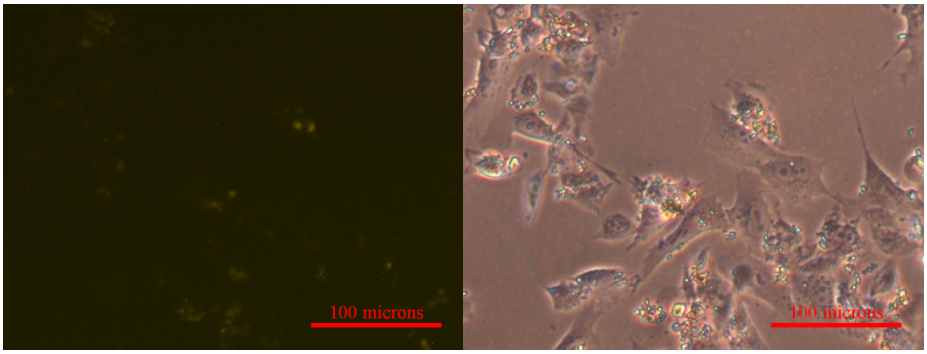

Figure S5. CLSM and bright field images showing of bone cancer cell line MG63 with FITC-MBG.

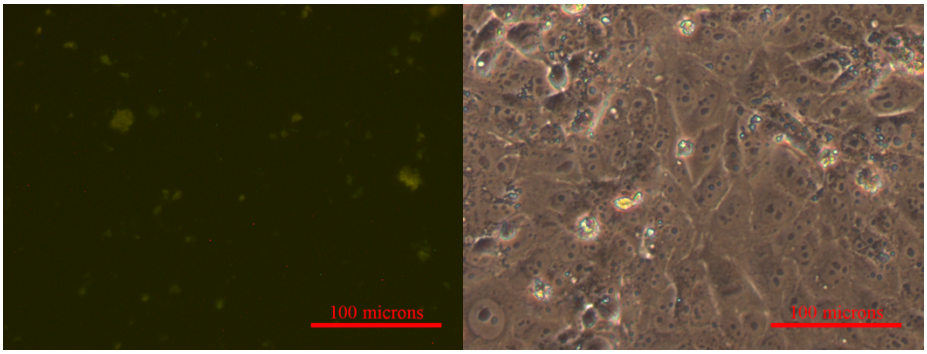

Figure S6. CLSM and bright field images showing of bone cancer cell line MG63 with FITC-MBG-FA.

We analyzed several concentrations to determine the IC50 value. As supporting figure 7, the effective of drugs have been analyzed. IC50 was determined by probit analysis using SPSS statistical software, version 10.0 (SPSS, Inc., Chicago, IL, USA) and refers to the concentrations of CPT, MBG/CPT and MBG-FA/CPT that cause a decrease in cell count by 50% in 24 hours, as determined from dose-response data.

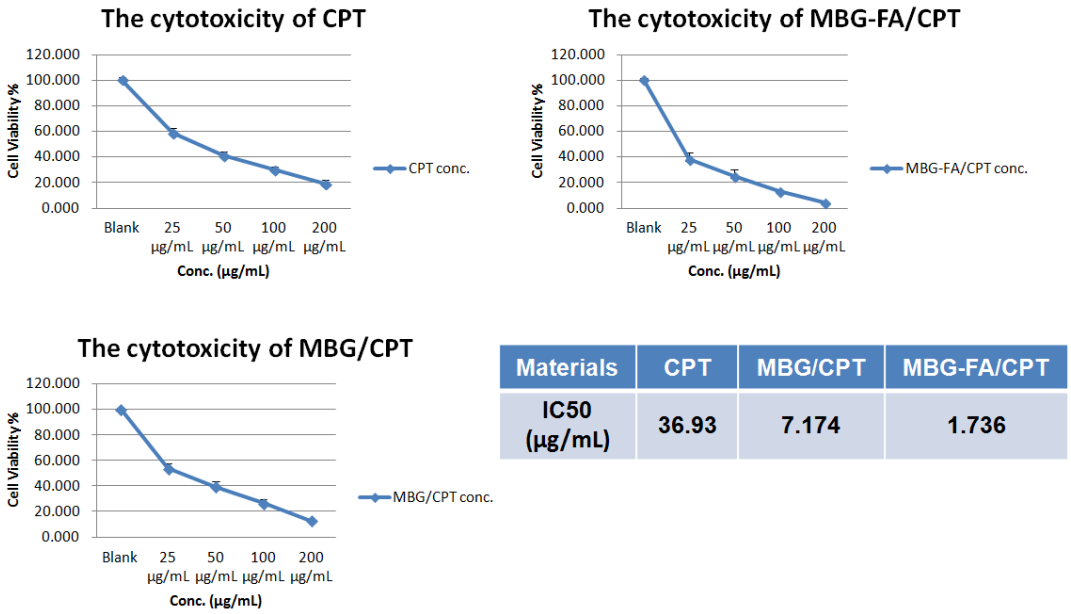

Materials	CPT	MBG/CPT	MBG-FA/CPT
IC50 (µg/mL)	36.93	7.174	1.736

Figure S7. Cyroroxicity tests of CPT, MBG/CPT and MBG-FA/CPT to HeLa cell lines after 24 h of incubation. IC50 was determined by probit analysis using SPSS statistical software.

At the figure S8, because MBG didn't sonicate 30 min before we test it on DLS, the size of MBG is about 5 μm. This result demonstrates that MBG may aggregate if we don't sonicate it.

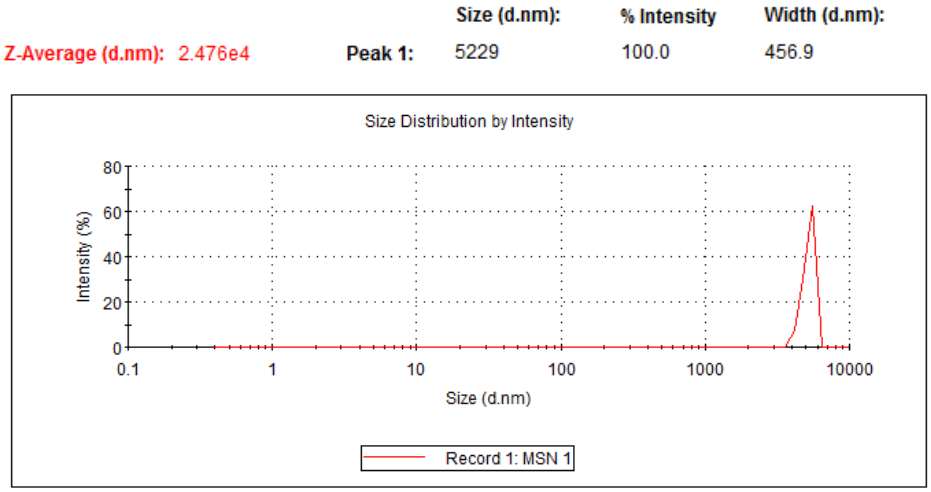

Figure S8. Dynamic light scattering data for MBG in water. In this process, MBG is not sonicated in water 30 min and it may combine into a larger particles.

But in the figure S2, the size of MBG is decreased and became 953 nm after we sonicate this sample 30 min in water. The reason why we test this data is because MBG will be sonicated while we are testing the cell experiment.

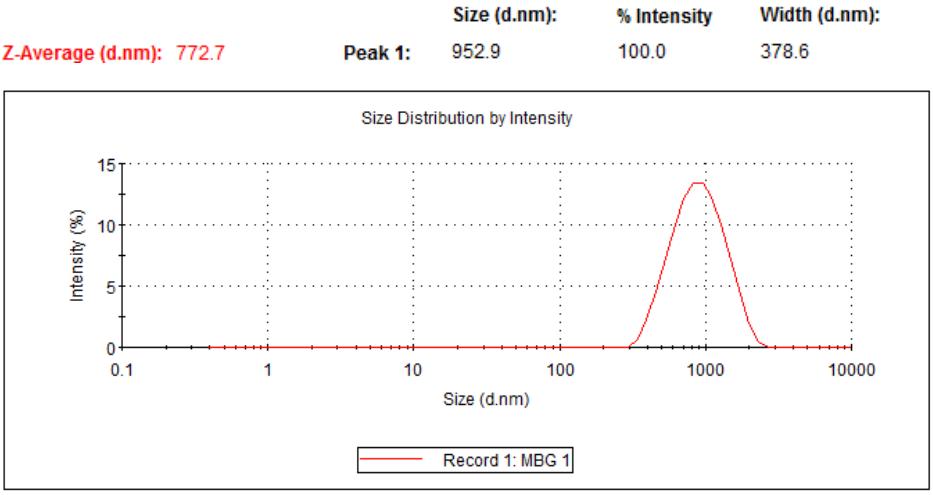

Figure S9. Dynamic light scattering data for MBG in water. In this process, MBG sonicated in water 30 min and divided into many fragments. The average size of MBG is about 0.9 nm.

In order to confirm whether MBG uptaken by cells or not, we design another experiment to try to explain the particle-linked FITC. In the new experiment section, HeLa and L929 cell lines were seeded at 2×10^5 cells per well into 6-well culture plates and incubated in DMEM for 24 h. The FITC-MBG and FITC-MBG-FA powder were added in medium with a concentration of 50 μg/mL. After soaking 3h, the MBG powder in medium was removed by centrifuge at 12000 rpm for 5 min, and the cells were treated with this medium at 37 °C with 5% CO_2. After 3 h of incubation, the medium was discarded, and the cells were washed twice with 2 mL of phosphate-buffered saline (PBS). Cells were then detached using a trypsin-EDTA solution and centrifuged at 2000 rpm for 10 min. The cells were resuspended in 2 mL of PBS, and 1×10^4 cell counts were immediately analyzed using a flow cytometer (FACSAria, BD). In addition, we compared the previous flow pattern with the new experiment. In the earlier flow pattern, it demonstrated an increase of fluorescent in the HeLa and L929 cells by MBG uptaken, and showed that the FITC could be detected by flow cytometer. However, when we choose the new experiment, flow cytometer cannot reveal the fluorescent data. This result display that even the MBG has been soaked in medium, the FITC was still linked on the surface of MBG.

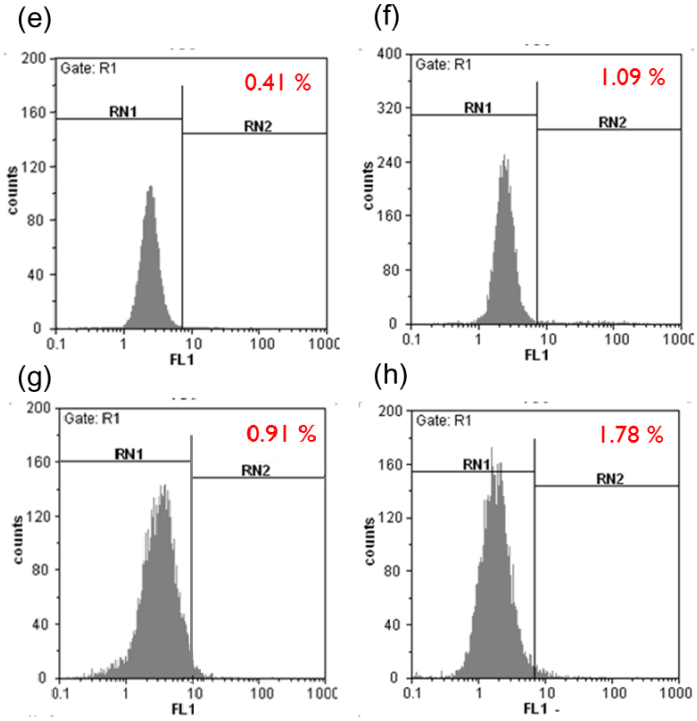

Fig. S10 Flow cytometry patterns of materials' endocytosis. Using the new experiment methods (e-h), the fluorescent does not shift to the RN2 region when we remove the MBG by centrifuge. Due to the fluorescent cannot be detected by flow, this result determine that the FITC molecules are conjugated on the surface of MBG indirectly.

Furthermore, we use this method to test if MBG can be detected by confocal. In the result, due to the MBG has been removed; the fluorescent cannot be identified.

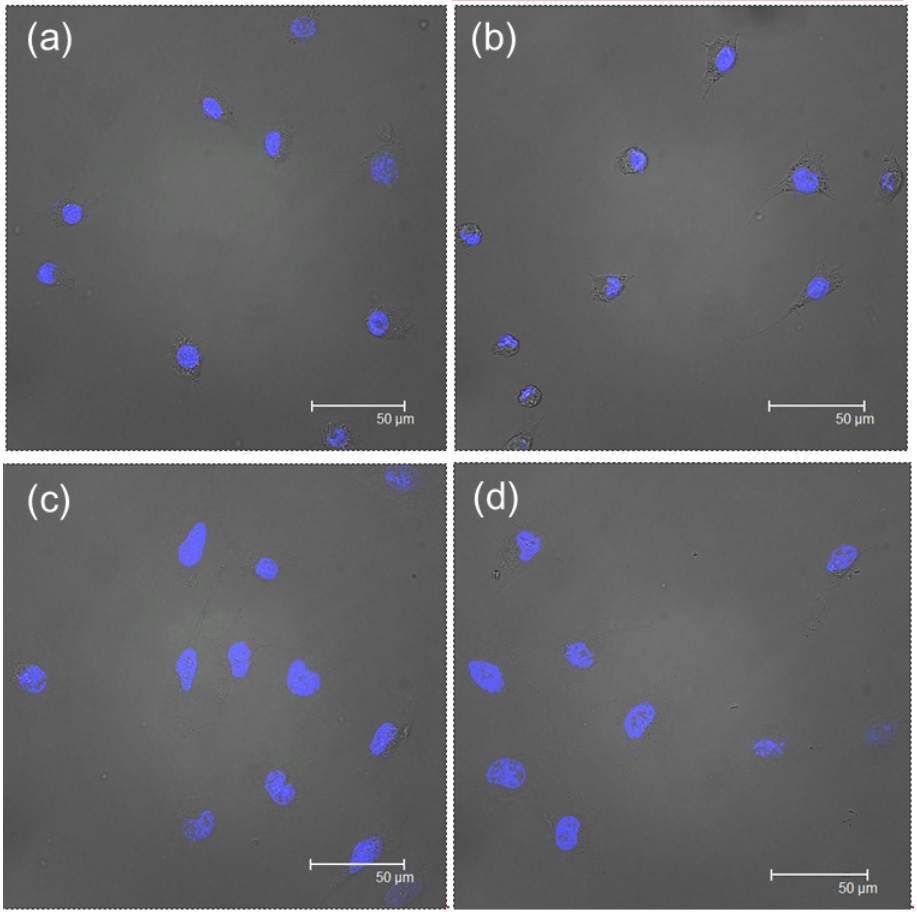

Fig. S11 CLSM images showing interaction of cancer cell line HeLa with (a) FITC-MBG, and (b) FITC-MBG-FA and of normal fibroblast cell line L929 with (c) FITC-MBG, and (d) FITC-MBG-FA after incubated 12 h. Even the MBG was soaked in medium 3h; the fluorescent cannot be detected after we removed MBG by centrifuge.

We can via the N_2 absorption/desorption measurement to see the change of pore volume or surface area before and after drug loading.

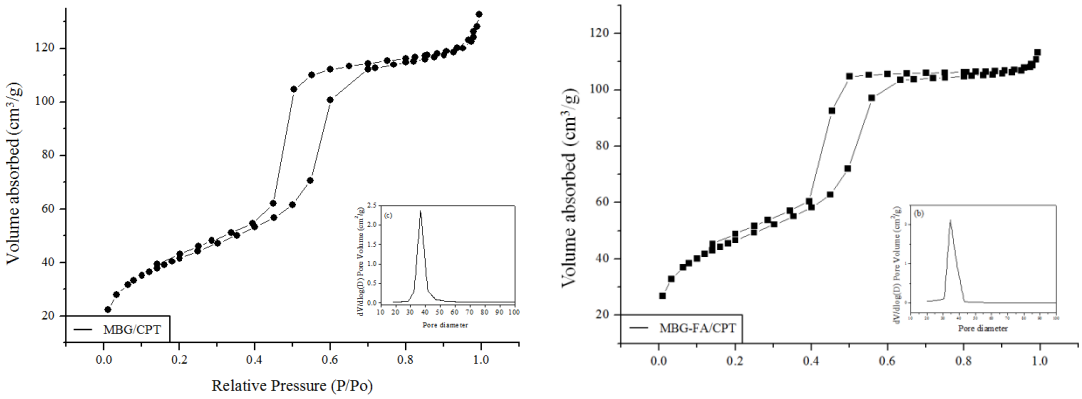

Sample	S_{BET} (m^2g^{-1})	V_P (cm^3g^{-1})	Pore size (nm)
MBG	671.72	0.89	5.4
MBG/CPT	21.752	0.026	3.6
MBG-FA	547.05	0.76	5.3
MBG-FA/CPT	54.412	0.061	3.3

Fig. S12 Nitrogen adsorption-desorption isotherms in MBG/CPT and MBG-FA/CPT. Comparing with MBG, the pore volume and surface area become smaller after the CPT loading.